

# 磷化銦基板上之線狀量子結構

研究生：林志昌

指導教授：李建平博士

國立交通大學

電子工程學系電子研究所

## 摘要

此篇博士論文利用固態源分子束磊晶系統，在與(100)磷化銦基板晶格匹配之砷化鎵銦與砷化鋁銦基材上，探討如何成長自組化砷化銦與砷化鎵線狀量子結構。並研究這些量子線狀結構的光學與電學特性，與探索利用作為元件的特性與價值。

一開始我們利用原子力顯微鏡技術，觀察在(100)磷化銦基板晶格匹配之砷化鎵銦基材上所成長的自組化砷化銦與砷化鎵量子結構形狀，以探討各種磊晶因素對這些量子結構型態的影響。在適當的磊晶條件下，砷化銦與砷化鎵量子結構都形成沿 $[1\bar{1}0]$ 方向的線狀量子結構。砷化銦與砷化鎵量子結構的成長行為有些不一樣，我們將分別對砷化銦與砷化鎵量子結構成長因素分別分析探討。

利用穿透式電子顯微鏡技術，所得之樣品截面圖中，發現(100)磷化銦基板晶格匹配之砷化鎵銦與砷化鋁銦基材上，所長的砷化銦與砷化鎵量子線，有堆疊行為。在砷化鎵銦基材，砷化銦與砷化鎵量子線皆為垂直堆疊，但在砷化鋁銦基材，砷化銦量子線是交叉堆疊，頗似體心立方結構。我們亦明顯觀察到基材中的組成調變現象。基於砷化鎵銦與砷化鋁銦基材中的週期性應變分佈，所造成的組成調變行為將分別在文章中探討。之後，利用組成調變現象，探討並解釋砷化銦與砷化鎵線狀量子結構的堆疊行為機制。

良好形狀之砷化銦量子線，在偏極化光激發光實驗中，發現有明顯之光學偏極化行為。電場平行於量子線的光激發光，其亮度大於電場垂直於量子線的光激發光。我們並利用磷化銦量子線做成半導體雷射元件，其雷射光波長約在1.7微米。為探討量子線之

異向性光學行為，分別沿 $[1\bar{1}0]$ 與 $[110]$ 方向，製作兩組不同雷射共振腔方向的樣品。從光功率電流 (L-I) 曲線與雷射光譜中，不同共振腔方向的雷射有極大的差異性。雷射對溫度相依的特性，也隨不同的共振腔方向而有不同，而且在共振腔垂直於量子線的雷射二極體中，出現從基態雷射狀態轉變到為激發態雷射狀態的行為。

我們亦對砷化銦量子線的電學傳輸行為做探討。砷化銦量子線包埋在砷化鎵銦與砷化鋁銦形成的異質介面附近。為了探討電子異向性傳輸行為，分別沿 $[1\bar{1}0]$ 與 $[110]$ 方向，製作兩組霍爾槓 (Hall bar) 樣品。霍爾量測從 10K 進行至室溫，結果顯示遷移率沿 $[1\bar{1}0]$ 與 $[110]$ 方向，有很大的差異性，傳輸通道平行於量子線的電子遷移率大於傳輸通道垂直於量子線的電子遷移率。這個異向性電子遷移率行為是由於量子線散射源不同方向的散射截面所造成。

最後，我們對論文作總結。量子線不只提供我們研究一維系統之光學與電學行為，並給出一些有趣的應用潛能。



# Wire-like Quantum Structures on InP Substrates

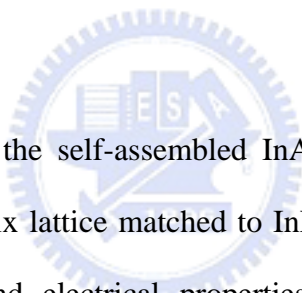
Student: Zhi-Chang Lin

Advisor: Dr. Chien-Ping Lee

Department of Electronic Engineer and Institute of Electronic Engineering

National Chiao Tung University

## Abstract



This dissertation studies the self-assembled InAs/GaAs wire-like quantum structures grown in InGaAs/InAlAs matrix lattice matched to InP substrates by solid source molecular beam epitaxy. The optical and electrical properties of these wire structures and their applications were explored.

This study begins with the investigation of growth conditions of self-assembled InAs and GaAs quantum structures in InGaAs matrix on (100) InP substrates. The morphology of the grown structures was studied by the atomic force microscopic technique. In a suitable growth condition, both InAs and GaAs formed wire-like quantum structures elongated along  $[1\bar{1}0]$  direction. However, the growth behaviors for the InAs wires and the GaAs wires are different. The growth parameters that influence the formation of InAs and GaAs are discussed.

By the cross-sectional transmission electron microscopic technique, the stacking behaviors of InAs/GaAs nano wires in InGaAs/InAlAs matrix on (100) InP substrates were

studied. In the InGaAs matrix, InAs and GaAs wires are vertically aligned. However, the InAs wires in InAlAs matrix are arranged in a cross staggered pattern, similar to a b.c.c. structure. The composition modulation caused by the periodic strain distribution was observed. Based on the composition modulation, the mechanism of the stacking behaviors of InAs/GaAs nano wires were explained.

The polarization dependence photoluminescence of well-formed InAs quantum wires was investigated. The results show obvious anisotropy in the light polarization. The intensity of the light with its electric field polarized parallel to the wires is stronger than that with the electric field perpendicular to the wires. The InAs quantum wires were then utilized for laser application. The lasing wavelength is about 1.7  $\mu\text{m}$ . In order to investigate the anisotropic optical behavior, two laser cavity directions, along  $[1\bar{1}0]$  and  $[110]$ , were both fabricated. From the L-I curves and the lasing spectra, lasers in two orientations have obvious different behaviors. The temperature dependence of the lasing behaviors is also found to be dependent on the cavity orientations. Transition from the ground state lasing to the excited state lasing is observed when the quantum wires are perpendicular to the laser cavity.

The electrical transport property of InAs quantum wires was also investigated. The InAs quantum wires were embedded in the InGaAs/InAlAs heterostructure. In order to measure the electron anisotropic transport behavior, two sets of Hall bar samples with orientations along  $[1\bar{1}0]$  and  $[110]$  directions were fabricated. Hall measurement, from 10K to room temperature, show that the mobilities along  $[1\bar{1}0]$  and  $[110]$  directions are very different. When the conduction channel is parallel to the quantum wires, the mobility is much higher than the mobility when the conduction channel is perpendicular to the wires. This mobility anisotropy is explained by the difference in the cross section of the scattering centers caused by wires.

Finally, the conclusion of this thesis research is given. The nano wires not only provide a medium for us to study the optical transition and the transport in one-dimensional systems, but also provide opportunities for interesting device applications.



## 致謝

這個博士班的歷程，要感謝的人太多太多了。尤其到最後完成的階段，陷入困境，沒有他們的諒解，支持，與陪伴，幫我解決許多困難，我現在應還在困境中奮鬥。有太多人要感謝了。

首先要感謝的，是我的指導教授：李建平教授，由於他的潛移默化，在他身上，我學到許多事情，如對事情的處理態度，與人相待的幫忙關懷，對學術的熱誠。一件事不得不提，老師放手要求讓學生獨立研究與對學術上的嚴厲要求，最後竟讓我徹底走出我的困境，雖然有點矛盾，但卻是事實。很感謝老師在最後對學生處於最糟糕時的諒解與支持。沒有老師你，我不知道何時才能走出十年前開始困擾我的狀態。雖然到博士班最後，才真正走出困境並開始領略到獨立做研究的真正樂趣與成就，已經有點遲了，但這些經驗，已是最寶貴的資產，一輩子都將跟著我。

再來要感謝的是林聖迪教授，與你共事的時間雖只有博士班最初三年左右，但在你身上，我感受到你對周遭人們的關心與愛護，對責任事物的嚴格要求，還有對學術的熱忱，跟你討論，總讓我學到東西，在你身上，我亦觀摩到許多東西，很感謝你指點我許多學術上的研究，並包容我一些奇怪堅持。而顏順通教授在我博士班求學過程中，總是不斷帶領我關心我，並讓我看到顏教授那股對學術的熱愛與高度要求，你的風範，總讓我仰慕。另外李秉奇博士是跟我共事 MBE 與其他研究最久的學長，那段為 MBE 機台奮鬥的記憶與一堆研究設備的架設維護經驗，還有跟你討論學術的記憶，讓我印象深刻。呂佳穎學妹，是我唯一親身帶的碩士班優秀學妹，與你共事的那一年多，永遠陽光的你，總是給我鼓勵，還有那段一起為雷射實驗，拼了老命一直熬夜奮鬥做實驗的甘苦回憶，將是一輩子的回憶。吳正信教授在我博士班後半段期間，給了我許多寶貴意見，尤其最後一兩年，更與我討論許多磊晶與實驗的問題，亦給我許多關懷，還有你對人對事的態度，總讓我獲益良多。此外亦感謝奈米科技中心副主任孫建文教授在光學量測上的指點。中興大學的孫允武教授，謝文興博士，李良箴博士，跟你們實驗室合作是一段很美好的回憶，而且孫教授與謝博士對我的關懷幫助，我銘記在心。還有許多人，如林國瑞教授在雷射上與 MBE 上的指導，還有黃忠諤博士，蔡富義博士，邱舒偉博士，黃坤宇博士，李漢傑博士，李建騏博士，廖志豪博士，與別實驗室的朋友：呂函庭博士，張晃崇博士，張尚文博士，楊宗禧博士，感謝攻讀博士時跟你們共事與討論的日子。博士班的學弟：王興燁，黃世傑，羅明城，凌鴻緒，林大鈞，跟你們一起維修保養 MBE，一起使用維護實驗室其他設備，互相討論研究，互相打氣的回憶，是段美好的回憶。還有歷屆的碩士班學弟妹們，與你們一起共事奮鬥，一起聊天出玩，還有互相幫忙打氣加油的日子，因為你們，常給我動力與支持。還有以前我念碩士班時的周亞謙教授，張振義博士，感謝你們領我進入學術領域並不斷鼓勵支持那時深深陷入低潮的我，並盡量拉我出來。

還有一些衛道中學，清華大學物理系的朋友與師長們，人生路上，你們的陪伴，支持，交心，有人甚至只是一句話，就可以不辭辛勞的給予幫忙或陪伴。心中將永遠惦記

一些人對我的付出。其中一人不得不提，那就是新加坡國立大學梁耕僑教授，我大學時的好友，他不辭辛勞花費許多時間，幫我校改博士論文英文稿，並給予我許多英文寫作的寶貴意見，這本博士論文多虧他勞心勞力幫忙，才得以順利完成。

我的家人，弟弟與弟媳你們兩人，在我最困難的時候，你們既使在萬忙之中，也要抽空來幫我，並盡一切力量幫我，我心中對你們的關懷幫助，深深感動，再多的感謝也無以說出我對你們的感謝。也要感謝一些親戚對我的關懷與鼓勵。還有已往生的爺爺，感謝我年幼時，你對我無止盡的關懷照顧。最後是養我育我的爸媽，沒有你們，就沒有今天的我，我今天所有的成就都是你們辛勞的結果。你們對我的任何抉擇，總是信任尊重與包容，讓我可以盡情選我喜歡的人生道路。你們的身教言教，總讓我學習，尤其你們的關心照料與不求回報的無止盡付出，讓我深深感動。用此論文，感謝爸媽的教養。

最後，感謝所有幫助過我的人，深深獻上感恩與祝福，謝謝你們。



# Contents

<b>Chinese Abstract.....</b>	<b>i</b>
<b>English Abstract.....</b>	<b>iii</b>
<b>Acknowledgement.....</b>	<b>vi</b>
<b>Content.....</b>	<b>viii</b>
<b>Table Caption.....</b>	<b>xi</b>
<b>Figure Caption.....</b>	<b>xii</b>
<b>Chapter 1: Introduction.....</b>	<b>1</b>
<b>Chapter 2: Experimental Techniques.....</b>	<b>9</b>
<b>2.1: Introduction.....</b>	<b>9</b>
<b>2.2: Molecular Beam Epitaxy.....</b>	<b>9</b>
<b>2.3: Material Characteristic Analysis.....</b>	<b>19</b>
<b>2.4: Device Processes.....</b>	<b>25</b>
<b>2.5: Device Measurements.....</b>	<b>26</b>
<b>Chapter 3: InAs/GaAs Quantum Structure Growth in InGaAs Matrix on     InP Substrate.....</b>	<b>30</b>
<b>3.1: Introduction.....</b>	<b>30</b>
<b>3.2: InAs Quantum Structure Growth in InGaAs Matrix on InP Substrates....</b>	<b>31</b>
<b>3.3: GaAs Quantum Structure Growth in InGaAs Matrix on InP Substrates...</b>	<b>39</b>
<b>3.4: Summary.....</b>	<b>48</b>



<b>Chapter 4: Ordering of Stacked InAs/GaAs Nano Wires in InGaAs/InAlAs</b>	
<b>Matrix on (100) InP Substrates.....</b>	49
<b>4.1: Introduction.....</b>	49
<b>4.2: Epitaxy Structures.....</b>	50
<b>4.3: Transmission Electron Microscope Results.....</b>	51
<b>4.4: Explanation for Stacking Behaviors of Wire-like Quantum Structures.....</b>	59
<b>4.5: Summary.....</b>	61
<b>Chapter 5: Self-Assembled InAs Quantum Wire Lasers.....</b>	63
<b>5.1: Introduction.....</b>	63
<b>5.2: Theories of Quantum Wires.....</b>	64
<b>5.3: The Epitaxy Structure and Processes of Quantum Wire Laser Diodes.....</b>	68
<b>5.4: Polarization Dependent Photoluminescence.....</b>	71
<b>5.5: Lasing Spectra.....</b>	75
<b>5.6: L-I Curves.....</b>	83
<b>5.7: Summary.....</b>	87
<b>Chapter 6: Mobility Asymmetry in InGaAs/InAlAs Hetrostructures with</b>	
<b>InAs Quantum Wires.....</b>	89
<b>6.1: Introduction.....</b>	89
<b>6.2: Epitaxy Structures and Hall measurement.....</b>	90
<b>6.3: Sheet Carrier Concentration.....</b>	92
<b>6.4: Electron Hall Mobility.....</b>	96
<b>6.5: Summary.....</b>	97
<b>Chapter 7: Conclusion and Future Work.....</b>	99

<b>7.1: Conclusion of Present Work.....</b>	<b>99</b>
<b>7.2: Future Work.....</b>	<b>102</b>
<b>Reference.....</b>	<b>104</b>
<b>Vita.....</b>	<b>111</b>
<b>Publication List.....</b>	<b>112</b>



## Table Captions

Table 3.1: List of InAs quantum structure growth condition

Table 3.2: List of GaAs quantum structure growth condition



## Figure Captions

Fig.1.1: The density of states: (a) Bulk. (b)Quantum well. (c)Quantum wire. (d)Quantum dot.

Fig.1.2: The sketches of lattice-mismatched growth modes: (a) Frank-van der Merwe mode.

(b)Volmer-Weber mode. (c)Stranski-Krastannow mode.

Fig.1.3: (a)Two types of the identifying flats on the 2" (100) InP wafers. (b) the diagram

shows that  $(h,k,l) = [h,k,l]$  for the cubic crystal system.

Fig.2.1: The sketch of Veeco Varian GEN II solid source MBE system

Fig.2.2: The atomic mechanism of the crystal deposition

Fig.2.3: The formation of the RHEED oscillation. (Ref.65)

Fig.2.4: The RHEED oscillation obtained by a Ga cell

Fig.2.5: The schematic picture of the HRXRD. (Ref.67)

Fig.2.6: The HRXRD spectrum results for lattice matched to InP check (a)InGaAs (b)InAlAs

Fig.2.7: A diagram of the AFM operation principle

Fig.2.8: (a)The scheme of the PL measurement system. (b) The scheme of the PPL

measurement system, modified from the PL system.

Fig.2.9: Two geometry types for Hall effect measurement: (a) long, narrow 8-contact Hall bar

geometry. (b) Nearly square Van der Pauw geometry

Fig.2.10: Temperature dependence for laser diode L-I curve measurement system

Fig.2.11: The Temperature Dependence Spectrum analyzer for laser diodes

Fig.2.12: The longitudinal mode spectrum of a QWR laser diode measured by the spectrum

analyzer in Fig.2.11

Fig.3.1: InAs quantum structure dependence on the InAs monolayer number: (a)

2ML(Lm4009). (b) 3ML(Lm4237). (c) 4ML(Lm4249). (d) 5ML(Lm4250). (e)  
6ML(Lm4264). (f) 8ML(Lm4265).

Fig.3.2: InAs quantum structure dependence on the substrate temperature: (a) 525 (Lm4249).  
(b) 515 (Lm4283). (c) 520 (Lm4330). (d) 510 (Lm4547).

Fig.3.3: InAs quantum structure dependence on As<sub>2</sub> BEP: (a) 2.5E-6torr (Rn0072). (b)  
1.5E-6torr (Rn0084).

Fig.3.4: InAs quantum structure dependence on the In growth rate and the interruption time:  
(a) 0.056μm/hr with 10sec interruption (Rn0072). (b) 0.55μm/hr without interruption  
(Rn0073).

Fig.3.5: GaAs quantum structure dependence on GaAs monolayer number at 510 : (a) 2ML  
(Lm3795). (b) 3ML (Lm3796). (c) 4ML (Lm3797).

Fig.3.6: GaAs quantum structure dependence on GaAs monolayer at 525 : (a) 3ML  
(Lm4071). (b) 2.5ML (Lm4095). (c) 3.5ML (Lm4096).

Fig.3.7: GaAs quantum structure dependence on substrate temperature: (a) 525 (Lm4071).  
(b) 510 (Lm4101). (c) 500 (Lm4102). (d) 515 (Lm4108). (e) 505 (Lm4109).  
(f) 510 (Lm4122).

Fig.3.8: GaAs quantum structure dependence on As<sub>2</sub> BEP: (a) As<sub>2</sub> BEP~1E-6torr (Lm4145).  
(b) As<sub>2</sub> BEP~2E-6torr (Lm4376).

Fig.3.9: GaAs quantum structure dependence on the interruption time: (a) Without  
interruption (Lm4122). (b) 60sec interruption between monolayer (Lm4142).

Fig.4.1: The sketch of the epitaxy structure

Fig.4.2: Cross-sectional TEM pictures of 3ML GaAs in InGaAs matrix: (a) (1 $\bar{1}$ 0) plane. (b)  
(110) plane.

Fig.4.3: Cross-sectional TEM pictures of 3ML InAs in InGaAs matrix: (a) (1 $\bar{1}$ 0) plane. (b)  
(110) plane.

Fig.4.4: Cross-sectional TEM pictures of 3.75ML in InAlAs matrix: (a)  $(1\bar{1}0)$  plane. (b)  $(110)$  plane.

Fig.4.5: (a) The cross-sectional HRTEM picture taken in the  $(1\bar{1}0)$  plane of stacked 3ML GaAs anti-QWrs in InGaAs matrix. (b): The cross-sectional HRTEM picture taken in the  $(1\bar{1}0)$  plane of stacked 3ML InAs QWrs in InGaAs matrix. (c): The cross-sectional HRTEM picture taken in the  $(1\bar{1}0)$  plane of stacked 3.75ML InAs QWrs in InAlAs matrix

Fig.4.6: Composition modulation phenomena: (a) Single period of 3ML GaAs anti-QWrs in InGaAs matrix. (b) Single period of 4.5ML InAs QWrs in InGaAs matrix. (c) Three periods of 3.75ML InAs QWrs in InAlAs matrix.

Fig.4.7: Composition modulation and formation of ordered nano wires in different material systems: (a) GaAs anti-QWrs in InGaAs matrix. (b) InAs QWrs in InGaAs matrix. (c) InAs QWrs in InAlAs matrix.

Fig.5.1: The rectangular quantum wire

Fig.5.2: The epitaxy structure of the QWr laser

Fig.5.3: The process flow of QWr laser diodes

Fig.5.4: PPL results: (a)20K. (b)40K. (c)80K. (d)100K. (e)120K. (f)140K. (g)160K. (h)180K. (i)200K. (j)220K. (k)240K.

Fig.5.5: The PL peak wavelength and the polarity at different temperatures of the InAs QWrs

Fig.5.6: Lasing wavelength vs. temp. for QWr lasers with the cavity QWrs

Fig.5.7: The comparison among PL spectra, lasing spectra of the laser cavity QWrs, and the laser cavity // QWrs at (a) 20K. (b) 40K. (c) 80K. (d) 100K. (e) 120K.

Fig.5.8: Lasing spectrum vs. current for QWr laser with the cavity QWrs at T=140K: (a)35mA. (b)60mA. (c)80mA.

Fig.5.9: Lasing spectrum vs. current for QWr laser with the cavity QWrs at T=160K:

(a)65mA. (b)100mA. (c)230mA.

Fig.5.10: Lasing spectrum vs. current for QWr laser with the cavity QWrs at T=180K:

(a)110mA. (b)180mA. (c)270mA.

Fig.5.11: Lasing spectrum vs. current for QWr laser with the cavity QWrs at T=200K:

(a)140mA. (b)230mA. (c)310mA.

Fig.5.12: Outlines of the explanation for the ground state lasing to the exciting state lasing transition: (a)T<140K.(b)T=140K.(c)T=160K.(d)T>160K.

Fig.5.13: L-I curves at different temperatures. (a)the laser cavity QWrs. (b)the laser cavity // QWrs.

Fig.5.14:  $I_{th}$  vs. temp. for the laser cavity // QWrs and for the laser cavity QWrs. The  $I_{th}$  ratio vs. temp. is also plotted

Fig.6.1: The InGaAs/InAlAs heterostructures prepared in this study: Sample A had no InAs QWrs; Sample B had an extra InAs QWrs 3nm below the heterointerface; Sample C had the InAs QWrs right at the interface.

Fig.6.2: The epitaxy structure of Sample D.

Fig.6.3: The electron mobility and sheet carrier density as functions of temperature for Sample A, Sample B, and Sample C, parallel and perpendicular to the InAs QWrs

Fig.6.4: The electron mobility and sheet carrier density as functions of temperature for Sample D, with 2.6 InAs QDs, in  $[110]$  and  $[1\bar{1}0]$  directions.

Fig.6.5: The AFM image of Sample D.

Fig.6.6: The electron mobility ratio as a function of temperature for Sample B and Sample C.